QUT Digital Repository:
http://eprints.qut.edu.au/

This is the author version published as:

Majumder, Ritwik and Ledwich, Gerard and Ghosh, Arindam and Zare, Firuz (2010) *Droop control of converter interfaced micro sources in rural distributed generation.* IEEE Transactions on Power Delivery.

# Droop Control of Converter Interfaced Micro Sources in Rural Distributed Generation

Ritwik Majumder, *Student Member, IEEE*, Gerard Ledwich, *Senior Member, IEEE*,
Arindam Ghosh, *Fellow, IEEE*, Saikat Chakrabarti *Member, IEEE* and Firuz Zare, *Senior Member, IEEE*

*Abstract*: **This paper proposes new droop control methods for load sharing in a rural area with distributed generation. Highly resistive lines, typical of rural low voltage networks, always create a big challenge for conventional droop control. To overcome the conflict between higher feedback gain for better power sharing and system stability in angle droop, two control methods have been proposed. The first method considers no communication among the distributed generators (DGs) and regulates the converter output voltage and angle ensuring proper sharing of load in a system having strong coupling between real and reactive power due to high line resistance. The second method, based on a smattering of communication, modifies the reference output voltage angle of the DGs depending on the active and reactive power flow in the lines connected to point of common coupling (PCC). It is shown that with the second proposed control method, an economical and minimum communication system can achieve significant improvement in load sharing. The difference in error margin between proposed control schemes and a more costly high bandwidth communication system is small and the later may not be justified considering the increase in cost. The proposed control shows stable operation of the system for a range of operating conditions while ensuring satisfactory load sharing.**

*Index Terms*: **Autonomous microgrid, Angle droop, Active and reactive Power sharing, Resistive lines.**

## I. INTRODUCTION

IN AN AUTONOMOUS microgrid, load sharing without communication between converters is the most desirable option as the network can be complex and can span over a large geographic area. A common approach to achieve this is through the use of frequency droop characteristics so that the parallel converters can be controlled locally to deliver desired real and reactive power to the system. The real and reactive power sharing can be achieved by controlling two independent quantities – the frequency and the fundamental voltage magnitude [1]. In case of voltage source converter (VSC) based DGs, the output angle can be changed instantaneously and so drooping the angle is a better way to share load [2]. Frequency regulation constraint limits the allowable range of frequency droop gain, which in turn, may lead to chattering during frequent load changes in a microgrid. Therefore the angle droop is adopted in this paper, which requires signals from global positioning system (GPS) for angle referencing, but no communication link between converters. While in [2], it is assumed the lines are mainly resistive and conventional droop can work with real power controlled by voltage and reactive power by angle, in this paper a high R/X ratio is considered, which is common in a rural network. With a strong coupling

R. Majumder, G. Ledwich, A. Ghosh, S. Chakrabarti and F. Zare are with the School of Engineering Systems, Queensland University of Technology, Brisbane, Australia.

of real and reactive power, they can not be controlled independently with either frequency or voltage and so the droop equations need to be modified. The real power droop coefficients can be chosen depending on the load sharing ratio. Moreover, the inclusion of linear quadratic regulator based state feedback controller makes reference following effective and shows a faster convergence compared to the frequency droop. In either of the case, frequency or angle droop, the output feedback gains have impact on system stability [3-5]. Transient stability of a power system with a high penetration of power electronics interfaced distributed generation is explored in [5]. In [4], small-signal stability analysis of load sharing control of multiple distributed generation systems (DGs) in a stand-alone ac supply mode is discussed.

Rural electrification relates to the availability of electricity for use by rural communities irrespective of the technologies, sources and forms of generation and has been the concern of the governments in many developing countries. However, it is often difficult to install extensive distribution network, especially since the customer density in the rural areas can be sparse. Distributed generation is one of the best available solutions for such a predicament. Planning of a typical medium-voltage rural distribution system in different loading conditions is discussed in [6]. The bottom up approach through an evaluation of autonomous or non-autonomous modified microgrid concept to provide electricity to local residents is proposed in [7].

In the rural areas where the distribution is in low or medium voltage, the lines are highly resistive and the resistance may be high enough to challenge the power sharing controller efficacy. High values of feedback gains are required to ensure proper load sharing, especially under weak system conditions. However, high gains have a negative impact on overall stability of the system. Moreover, proper sharing of load cannot be ensured even with high gain if the lines are highly resistive.

In [8], the decoupling of the real and reactive power is achieved for a high R/X line with frequency droop control. It is shown that a modifying the droop equation can accommodate the effect of line impedance. However, the choice of droop gains for rating based sharing of power is not been addressed in [8].

The off grid renewable connection at Anangu Solar Station of south Australia [9], where 220 kW power is distributed covering 10,000 square km among number of communities up to 500 people or minigrid connection at Hermannsburg in central Australia [9], where three communities each with several hundred household with 720 kW total power consumption are the example of the discussed scenario where the converter interfaced micro sources and loads are geographically far from each other in a low voltage network.

Two methods have been proposed in this paper for power sharing with VSC connected DGs. In first method, decentralized operation of DGs without any communication is investigated. A transformation matrix is derived for control parameters and feedback gains taking into consideration the R-by-X ratios of the lines. In second method, the angle droop power sharing controller is modified to accommodate the highly resistive line. The reference angle of each converter output voltage is modified based on the desired active and reactive power flow and the line impedances. A minimum amount of communication is needed among the DGs for the change in reference angle of the output voltage. We have assumed a low-cost web-based communication system [10-12] for this purpose.

The contribution of the paper is the development of a graduated set of control algorithms to deal with different levels of communication infrastructure to support the microgrid with particular emphasis on highly resistive lines. The accuracy of the controllers is shown in different weak system conditions where the conventional angle droop fails to share the power as desired due to high coupling between the real and reactive power. Mathematical derivations and time domain simulations are used to illustrate the methodologies.

## II. POWER SHARING WITH ANGLE DROOP AND PROPOSED DROOP CONTROL

Notations for the line parameters and their normalized values are given below.

| | |
|---|---|
| $X_D$ | Line reactance |
| $X_L$ | Normalized line reactance |
| $X$ | Normalized filter reactance |
| $R_D$ | Line resistance |
| $R$ | Normalized line resistance |

To show the power sharing with angle droop, a system of two DGs with a load is considered as shown in Fig. 1. The voltages and the power flow are defined in the figure. Applying dc load flow with all the necessary assumptions [13], we get

$$\begin{aligned} \delta_1 - \delta &= (X_1 + X_{L1})P_1 \\ \delta_2 - \delta &= (X_2 + X_{L2})P_2 \end{aligned} \quad (1)$$

where $X_1 = \omega L_{f1}/(V_1 V_{11})$ , $X_{L1} = \omega L_{D1}/(V_{11}V)$, $X_2 = \omega L_{f2}/(V_2 V_{22})$ and $X_{L2} = \omega L_{D2}/(V_{22}V)$.
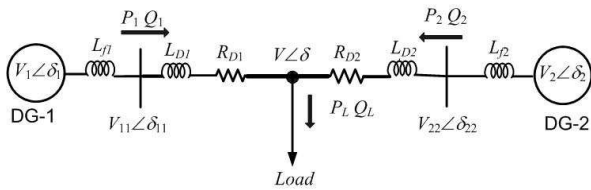


Fig. 1. Power sharing with angle droop.

The angle droop equation of the DGs are given by

$$\begin{aligned} \delta_1 &= \delta_{1rated} - m_1 \times (P_1 - P_{1rated}) \\ \delta_2 &= \delta_{2rated} - m_2 \times (P_2 - P_{2rated}) \end{aligned} \quad (2)$$

The ratio of the droop gains $m_2{:}m_1$ is chosen as the ratio of the rated power $P_{1rated}{:}P_{2rated}$, The rated droop angles are taken as $\delta_{1rated} = m_1 P_{1rated}$; $\delta_{2rated} = m_2 P_{2rated}$. Then from (2) we get

$$\delta_1 - \delta_2 = m_2 P_2 - m_1 P_1 \quad (3)$$

Similarly from (1) we get

$$\delta_1 - \delta_2 = (X_1 + X_{L1})P_1 - (X_2 + X_{L2})P_2 \quad (4)$$

From (3) and (4) we get,

$$\begin{aligned} (X_1 + X_{L1})P_1 - (X_2 &+ X_{L2})P_2 = m_2 P_2 - m_1 P_1 \\ \Rightarrow \frac{P_1}{P_2} &= \frac{X_2 + X_{L2} + m_2}{X_1 + X_{L1} + m_1} \end{aligned} \quad (5)$$

It is to be noted that the value of $X_1$ and $X_2$ are small compared to the value of $m_1$ and $m_2$ when normalized to same unit. Hence we can write

$$m_1 \gg X_1 \gg X_{L1} \text{ and } m_2 \gg X_2 \gg X_{L2}$$

From (5) we can write

$$\frac{P_1}{P_2} \approx \frac{m_2}{m_1} = \frac{P_{1rated}}{P_{2rated}} \quad (6)$$

It is evident from (6) that the droop coefficients should be inversely proportional to the DG rating and also the droop coefficients play the dominant role in the power sharing. The error is further reduced by taking the output inductance ($L_{f1}$, $L_{f2}$) of the DGs inversely proportional to power rating of the DGs. The comparison between the performance of this angle droop and a conventional frequency droop [1] is shown in Appendix A.

The simple system, shown in Fig. 1, is used to show the power sharing. In a real system with number of DGs and loads in different location line impedance will have an impact on the load sharing. But for a microgrid within a small geographical area, the line inductance will never be very high. Moreover a high droop coefficient will always play a dominant role and share the power as desired with a very small deviation.

To control power flow explicitly from any of the DGs to the local bus (e.g., DG-1 and the bus with voltage $V_{11}\angle\delta_{11}$), an output inductance (e.g., $L_{f1}$) is required. This output inductance enables us to decouple the real and reactive power injection. We shall use this structure for controlling power flow with communication (the 2$^{nd}$ proposed method). However, in the 1$^{st}$ proposed method, the output inductance is assumed to be zero. In this control method, we do not require a decoupling of real and reactive power as will be explained in the next subsection. Also this control is based on the R/X ratio of the line and therefore the inclusion of output inductance will require the knowledge of the line length. Note that the output inductance can be taken as zero depending on the converter output filter structure, discussed in Section III.

### A. Proposed Controller-1 without Communication

As discussed before, in the rural distribution system, at the medium or low voltage level the lines are mostly resistive and the values of the line impedances are not negligible. In that case (1) is not valid. In this case we have assumed that the

DGs do not have any output inductance, in which case, Fig.1 is redrawn as shown in Fig. 2. Here the line reactance ($\omega L_D$) value is chosen to be the same as line resistance value $R_D$.
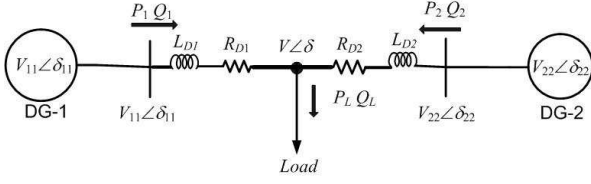


Fig. 2. Power sharing in resistive-inductive line.

The power flow from DG-1 for system shown in Fig.2 as

$$P_1 = \eta[R_{D1}(V_{11} - V\cos(\delta_{11} - \delta)) + X_{D1}V\sin(\delta_{11} - \delta)]$$
$$Q_1 = \eta[-R_{D1}V\sin(\delta_{11} - \delta) + X_{D1}(V_{11} - V\cos(\delta_{11} - \delta))]$$

where $\eta = V_{11}/(R^2{}_{D1} + X^2{}_{D1})$. From the above equation, multiplying $Q_1$ by $R_{D1}$ and subtracting the product from the multiplication of $P_1$ and $X_{D1}$ we get

$$X_{D1}P_1 - R_{D1}Q_1 = V_{11}V\sin(\delta_{11} - \delta) \tag{7}$$

In a similar way, we also get

$$R_{D1}P_1 + X_{D1}Q_1 = V_{11}^2 - VV_{11}\cos(\delta_{11} - \delta) \tag{8}$$

It is to be noted that DG-1 does not have any control over the load voltage magnitude and angle. Thus the linearization of (7) and (8) around the nominal values of $V_{110}$ and $\delta_{110}$ results in

$$X_{D1}\Delta P_1 - R_{D1}\Delta Q_1 = (V_{110}V)(\Delta\delta_{11} - \Delta\delta) + (\delta_{110}V)\Delta V_{11} \tag{9}$$
$$R_{D1}\Delta P_1 + X_{D1}\Delta Q_1 = (2V_{110} - V)\Delta V_{11} \tag{10}$$

where $\Delta$ indicates the perturbed value. From (9) and (10), the output voltage magnitude and angle of a DG-1 can be written in terms of real and reactive power as,

$$\begin{bmatrix} \Delta\delta_{11} - \Delta\delta \\ \Delta V_{11} \end{bmatrix} = K(V)\begin{bmatrix} \dfrac{X_{D1}}{Z_1} & -\dfrac{R_{D1}}{Z_1} \\ \dfrac{X_{D1}}{Z_1} & \dfrac{R_{D1}}{Z_1} \end{bmatrix}\begin{bmatrix} \Delta P_1 \\ \Delta Q_1 \end{bmatrix} = K(V)T\begin{bmatrix} \Delta P_1 \\ \Delta Q_1 \end{bmatrix} \tag{11}$$

where the impedance $Z_1$ and the matrix $K(V)$ are given by

$$Z_1 = \sqrt{R_{D1}^2 + X_{D1}^2} \qquad K(V) = Z_1\begin{bmatrix} V_{110}V & \delta_{110}V \\ 0 & 2V_{110} - V \end{bmatrix}^{-1}$$

Defining pseudo real and reactive power as

$$\begin{bmatrix} \Delta P_1' \\ \Delta Q_1' \end{bmatrix} = T\begin{bmatrix} \Delta P_1 \\ \Delta Q_1 \end{bmatrix}$$

equation (11) the control strategy can be chosen as

$$\begin{bmatrix} \Delta\delta_{11} \\ \Delta V_{11} \end{bmatrix} = K(1)\begin{bmatrix} \Delta P_1' \\ \Delta Q_1' \end{bmatrix} \tag{12}$$

The above equation forms the basis of modified droop sharing where the matrix $K(V)$ is approximated as $K(1)$ with the as-

sumption that bus voltage is constant at 1 per unit, giving an error in the control gain of less than 5%. This will have no significant effect on the power sharing. The load bus angle $\delta$ is not measurable at the DG end. The chosen control (12) will automatically correct for changes in $\delta$, while retaining the desired decoupling property.

The droop control equation for DG-1 is then written as

$$\delta_{11} = \delta_{11rated} - m_1' \times (P_1' - P_{1rated}')$$
$$V_{11} = V_{11rated} - n_1' \times (Q_1' - Q_{1rated}') \tag{13}$$

where the rated powers ($P_{1rated}'$, $Q_{1rated}'$) are also represented after multiplying the conversion matrix [T]. Similar transformation is also used for the rated powers of DG-2 as well. The droop gains of the both the DGs are also transformed by the matrix $T$ and are given by as

$$\begin{bmatrix} m_1' \\ n_1' \end{bmatrix} = T\begin{bmatrix} m_1 \\ n_1 \end{bmatrix} \text{ and } \begin{bmatrix} m_2' \\ n_2' \end{bmatrix} = T\begin{bmatrix} m_2 \\ n_2 \end{bmatrix} \tag{14}$$

where the real and reactive power droop coefficients are

$$\frac{m_2}{m_1} = \frac{P_{1rated}}{P_{2rated}} \text{ and } \frac{n_2}{n_1} = \frac{Q_{1rated}}{Q_{2rated}} \tag{15}$$

Then droop equation (13) can be expressed as,

$$\begin{bmatrix} \delta_{11} \\ V_{11} \end{bmatrix} = \begin{bmatrix} \delta_{11rated} \\ V_{11rated} \end{bmatrix} - T\begin{bmatrix} m_1 \\ n_1 \end{bmatrix}\begin{bmatrix} P_1' - P_{1rated}' \\ Q_1' - Q_{1rated}' \end{bmatrix} \tag{16}$$

This modified angle droop control not only ensures decoupling of the real and reactive power in a high R/X line, but also provide a rating based power sharing. The control of the output angle results in a much lower frequency deviation compared to frequency droop as shown in Appendix A.

*B. Proposed Controller-2 with Minimum Communication*

In this sub-section, a droop control is proposed that requires minimal communication. The system of Fig. 1 is considered here and the DGs are connected to the microgrid with their output inductances.

For small angle difference between the DGs and their respective local buses shown in Fig. 1, the power flow equations of the DGs are given by

$$\delta_1 - \delta_{11} = X_1 P_1$$
$$\delta_2 - \delta_{22} = X_2 P_2 \tag{17}$$

Both the active and reactive power flow in a highly resistive line are determined by angle difference in the terminal voltages. The power flow equations over the line for small angle differences can be written as

$$\delta_{11} - \delta = -R_1 Q_1 + X_{L1} P_1$$
$$\delta_{22} - \delta = -R_2 Q_2 + X_{L2} P_2 \tag{18}$$

where $R_1 = R_{D1}/(V_{11}V)$, $R_2 = R_{D2}/(V_{22}V)$, $X_{L1} = \omega L_{D1}/(V_{11}V)$ and $X_{L2} = \omega L_{D2}/(V_{22}V)$.

From (17) and (18) we get,

$$\delta_1 - \delta = X_1 P_1 - R_1 Q_1 + X_{L1} P_1$$
$$\delta_2 - \delta = X_2 P_2 - R_2 Q_2 + X_{L2} P_2 \qquad (19)$$

The difference between $\delta_1$ and $\delta_2$ is derived from (19) as

$$\delta_1 - \delta_2 = X_1 P_1 - R_1 Q_1 + X_{L1} P_1 - X_2 P_2 + R_2 Q_2 - X_{L2} P_2 \quad (20)$$

Again from (2) we get,

$$\delta_1 - \delta_2 = \delta_{1rated} - \delta_{2rated} - m_1 \times \left( P_1 - P_{1rated} \right)$$
$$+ m_2 \times \left( P_2 - P_{2rated} \right) \qquad (21)$$

Since the ratio of the droop gains $m_2{:}m_1$ is chosen as the ratio of the rated power $P_{1rated}{:}P_{2rated}$, from the above equation we get

$$\delta_1 - \delta_2 = \delta_{1rated} - \delta_{2rated} - m_1 P_1 + m_2 P_2 \qquad (22)$$

Equating (20) and (22) we get,

$$X_1 P_1 - R_1 Q_1 + X_{L1} P_1 - X_2 P_2 + R_2 Q_2 + X_{L2} P_2$$
$$= \delta_{1rated} - \delta_{2rated} - m_1 P_1 + m_2 P_2 \qquad (23)$$

The rated values of the converter output voltage angles are selected with active and reactive power output of the converter as

$$\delta_{1rated} = X_1 P_1 - R_1 Q_1 + X_{L1} P_1$$
$$\delta_{2rated} = X_2 P_2 - R_2 Q_2 + X_{L2} P_2$$

Substituting these values in (23), we get

$$m_1 P_1 = m_2 P_2 \quad \Rightarrow \frac{P_1}{P_2} = \frac{m_2}{m_1} = \frac{P_{1rated}}{P_{2rated}} \qquad (24)$$

It can be seen that the power sharing of the DGs are proportional to their rating. This control technique shown with above simple example can be extended to multiple DG system. This is discussed below.

*C. Multiple DG System*

Fig. 3 shows a multiple DG system where three DGs are connected at different location of the microgrid. The four loads that are connected to the microgrid are shown as *Load_1*, *Load_2*, *Load_3* and *Load_4*. The real and reactive power supply from the DGs are denoted by $P_i$, $Q_i$, $i = 1,\dots,3$. The real and reactive power flow for different line sections and load demand are shown in Fig. 3. The line impedances are denoted as $Z_{Di} (= R_{Di} + jX_{Di})$, $i = 1,\dots,6$. Each of the DG controllers needs to measure its local quantities only and hence,
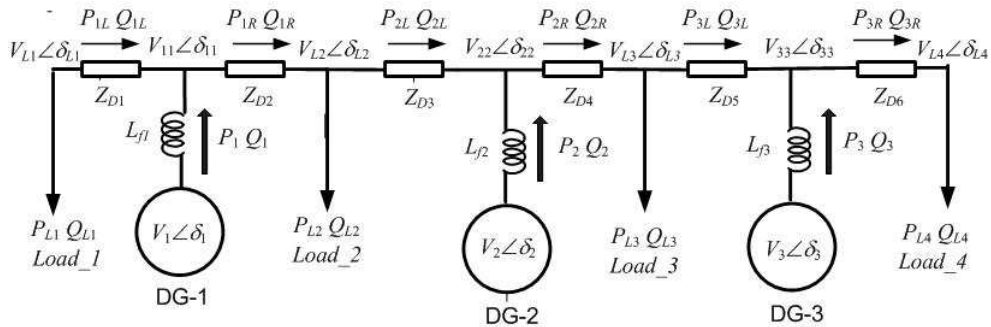
the real and reactive power flow measurements into and out of the DG local bus are required. It is to be noted all the line impedances and loads are assumed to be lumped.

From the power output of DG-3 we can write,

$$\delta_3 - \delta_{L4} = X_3 P_3 - R_6 Q_{3R} + X_{L6} P_{3R} \qquad (25)$$

where $R_6 = R_{D6}/(V_{33}V_{L4})$ and $X_{L6} = X_{D6}/(V_{33}V_{L4})$. Similarly from the DG-2 power output we can write,

$$\delta_2 - \delta_{L3} = X_2 P_2 - R_4 Q_{2R} + X_{L4} P_{2R} \qquad (26)$$

The angle difference between the loads can be represented as,

$$\delta_{L3} - \delta_{L4} = -R_5 Q_{3L} + X_{L5} P_{3L} - R_6 Q_{3R} + X_{L6} P_{3R} \qquad (27)$$

From (26) and (27) we get,

$$\delta_2 - \delta_{L4} = X_2 P_2 - R_4 Q_{2R} + X_{L4} P_{2R} - R_5 Q_{3L} + X_{L5} P_{3L}$$
$$- R_6 Q_{3R} + X_{L6} P_{3R} \qquad (28)$$

Similarly the power output of DG-1 can be expressed as,

$$\delta_1 - \delta_{L4} = X_1 P_1 - R_2 Q_{1R} + X_{L2} P_{1R} - R_3 Q_{2L} + X_{L3} P_{2L}$$
$$- R_4 Q_{2R} + X_{L4} P_{2R} - R_5 Q_{3L} + X_{L5} P_{3L} - R_6 Q_{3R} + X_{L6} P_{3L} \qquad (29)$$

It is to be noted that in (28) and (29), all the active and reactive power quantities, except the first term, are not locally measureable. The angle difference shown in (27) can be measured by DG-3 and then communicated to DG-2 and DG-1. As these quantities only modify the reference angle to ensure better load sharing, updates can be done using longer sample rates and a much slower communication process can achieve that. Furthermore, the first term in (28) and (29) indicates the primary output feedback loop that is based on the locally measurable power output of the DG. This control action is instantaneous and ensures initial load sharing among the DGs. We can write (29) as

$$\delta_1 - \delta_{L4} = \delta_{1p} + \delta_{11} + \delta_{12} + \delta_{13} \qquad (30)$$

where

$$\delta_{1p} = X_1 P_1, \quad \delta_{11} = -R_2 Q_{1R} + X_{L2} P_{1R}$$
$$\delta_{12} = -R_3 Q_{2L} + X_{L3} P_{2L} - R_4 Q_{2R} + X_{L4} P_{2R} \qquad (31)$$
$$\delta_{13} = -R_5 Q_{3L} + X_{L5} P_{3L} - R_6 Q_{3R} + X_{L6} P_{3L}$$



Fig. 3. Multiple DG connected to microgrid.

The longer updates can be made using a web based communication [11] that is discussed below.

It is to be noted that in this proposed method, there is a requirement of site specific tuning of the parameters for the reference angle generation. This tuning is required to improve the performance of the site independent decentralized control of Controller-1.

### D. Web Based Communication

The web based measurement system is shown in Fig. 4. The real and reactive power ($P$ and $Q$) measured at each DG unit is communicated to a dedicated website or company intranet with the help of a modem. Assuming that the PQ measurement units are already installed at each DG location, the equipment needed for each DG unit are a computer to collect the measurements from local and remote units, and a modem to transmit the measurements to the dedicated website, or to download remote measurements from it. Fig. 4 (a) shows the web connection of all the DGs, while the communication in each DG is shown in Fig. 4 (b). The power monitoring unit sends the real and reactive power measurement to the computer to calculate $\delta_{11}$ as shown in (31). The other angle component $\delta_{12}$ and $\delta_{13}$ are received by the modem and communicated to the DG control unit through the computer. As mentioned before the main load sharing term $\delta_{1p}$ in (30) is based on local measurement and so even in case of communication failure, a rough load sharing is ensured among the DGs. As the DGs are interfaced through converters, the structure and control of the converters are very important for the power sharing. They are discussed in the next section.
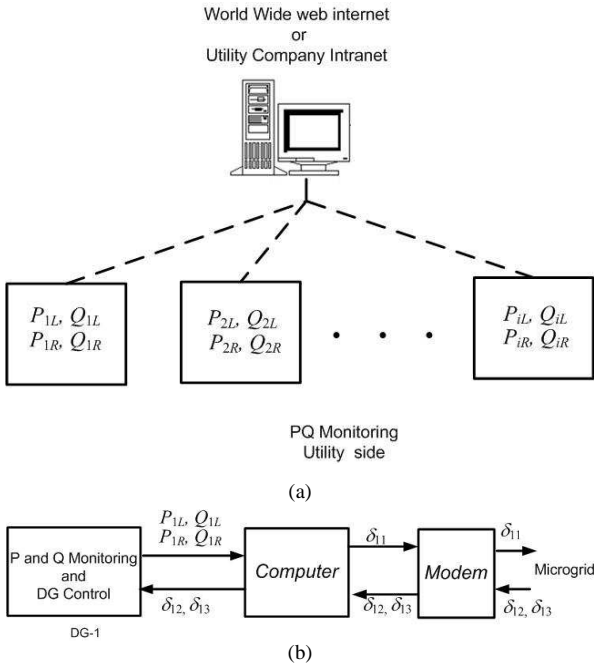


Fig. 4 (a) Web based PQ monitoring scheme and (b) web based communication for DG-1.

### III. CONVERTER STRUCTURE AND CONTROL

All the DGs are assumed to be an ideal dc voltage source supplying a voltage of $V_{dc}$ to the VSC. The structure of the VSC is shown in Fig. 5. The VSC contains three H-bridges that are supplied from the common dc bus. The outputs of the H-bridges are connected to three single-phase transformers that are connected in wye for required isolation and voltage boosting [14]. The resistance $R_T$ represents the switching and transformer losses, while the inductance $L_T$ represents the leakage reactance of the transformers. The filter capacitor $C_f$ is connected to the output of the transformers to bypass the switching harmonics, while $L_f$ represents the output inductance of the DG source.
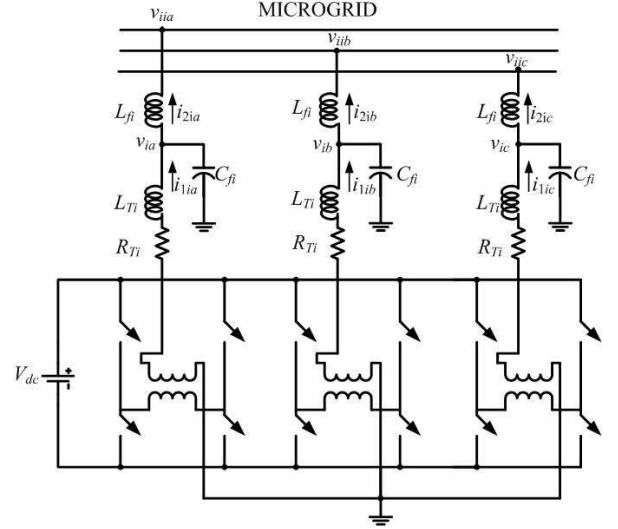


Fig. 5. Converter structure.

### A. Converter Control

The equivalent circuit of one phase of the converter is shown in Fig. 6. In this, $u \cdot V_{dc}$ represents the converter output voltage, where $u$ is the switching function and is given by $u = \pm 1$. The main aim of the converter control is to generate $u$. From the circuit of Fig. 6, the following state vector is chosen

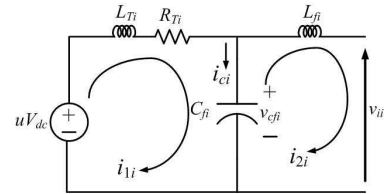$$z^T = \begin{bmatrix} i_1 & i_2 & v_{cf} \end{bmatrix} \tag{32}$$



Fig. 6. Single-phase equivalent circuit of VSC.

Then the state space equation of the system can be written as

$$\dot{z} = Az + Bu_c + Cv_{ii} \tag{33}$$

where $u_c$ is the continuous time approximation of the switching function $u$. and

$$A = \begin{bmatrix} -R_T/L_T & 0 & -1/L_T \\ 0 & 0 & 1/L_f \\ 1/C_f & -1/C_f & 0 \end{bmatrix}, B = \begin{bmatrix} V_{dc}/L_T \\ 0 \\ 0 \end{bmatrix}, C = \begin{bmatrix} 0 \\ -1/L_f \\ 0 \end{bmatrix}$$

The main aim of the converter control is to generate $u_c$ from a suitable state feedback control law such that the output voltage and currents are tracked properly according to their references. It is easy to generate references for the output voltage $v_{cf}$ and current $i_2$ from power flow condition. However, the same cannot be said about the reference for the current $i_1$. On the other hand, once the reference for $v_{cf}$ is obtained, it is easy to calculate a reference for the current $i_c$ through the filter capacitor (see Fig. 6).

To facilitate this, we define a new set of state vectors as

$$x^T = \begin{bmatrix} i_c & i_2 & v_{cf} \end{bmatrix} \tag{34}$$

We then have the following state transformation matrix

$$x = \begin{bmatrix} 1 & -1 & 0 \\ 0 & 1 & 0 \\ 0 & 0 & 1 \end{bmatrix} z = C_P z \tag{35}$$

The transformed state space equation is then given by combining (33) and (35) as

$$\dot{x} = C_p A C_p^{-1} x + C_p B u_c + C_p C v_{ii} \tag{36}$$

If the system of (36) is sampled with a sampling time of $\Delta T$, then its discrete-time description can be written in the form

$$x(k+1) = F x(k) + G u_c(k) + H v_{ii}(k) \tag{37}$$

To control the converter, we shall employ a discrete time line quadratic regulator which has the form

$$u_c(k) = -K \begin{bmatrix} x(k) - x_{ref}(k) \end{bmatrix}$$
$$= k_1 (i_{cref} - i_c) + k_2 (i_{2ref} - i_2) + k_3 (v_{cfref} - v_{cf}) \tag{38}$$

where $x_{ref}$ is the reference vector and $K$ is the feedback gain matrix obtained using discrete time linear quadratic regulator (LQR) with a state weighting matrix of $Q$ and a control penalty of $r$. From $u_c(k)$, the switching function is generated as

$$\text{If } u_c(k) > h \text{ then } u = +1$$
$$\text{elseif } u_c(k) < -h \text{ then } u = -1 \tag{39}$$

where $h$ is a small number. The above control action results in fairly accurate tracking [15]. This control strategy is applied to all the DGs, when operating with the web based communication of Section II.B.

The control law discussed so far is for the system in which the DGs have an output inductor. It can be seen from Fig. 5 that this implies the converter output stage has LCL (or T) filter structure. Alternatively, when the DGs do not have an output inductance, the inductance $L_{fi}$ is removed and the output filter is a simple LC filter. The system states are then modified as

$$x^T = \begin{bmatrix} i_{cf} & v_{cf} \end{bmatrix} \tag{40}$$

However the state space is similar to (32) and the control law (38) and switching logic (39) remain the same. This control strategy is applied to all the DGs, when operating without any communication of Section II.A.

It is assumed the total power demand in the microgrid can be supplied by the DGs and no load shedding is required. The output voltages of the converters are controlled to share this load proportional to the rating of the DGs as discussed in different droop control methods.

### B. DG Reference Generation

It is evident from (34) and (38) that references for all the elements of the states are required for state feedback. Since $V$ and $\delta$ are obtained from the droop equation, the reference for the capacitor voltage and current are given by

$$v_{cfref} = V \sin(\omega t + \delta) \tag{41}$$
$$i_{cfref} = V \omega C_f \sin(\omega t + \delta + 90°) \tag{42}$$

For the LCL filter, the reference for the current $i_2$ can be calculated as

$$i_{2ref} = |I_{2ref}| \sin(\omega t + \delta_{2ref}) \tag{43}$$

From Fig. 5, it can be seen that

$$|I_{2ref}| = \frac{\sqrt{P^2 + Q^2}}{V_{cf}} \text{ and } \delta_{2ref} = \delta - \tan^{-1}(Q/P)$$

TABLE-I: NOMINAL SYSTEM PARAMETERS

| System Quantities | Values |
|---|---|
| **Systems frequency** | 50 Hz |
| **Feeder impedance** | |
| $Z_{D1}$ | 1.0 + j 1.0 Ω |
| $Z_{D2}$ | 0.4 + j 0.4 Ω |
| $Z_{D3}$ | 0.5 + j 0.5 Ω |
| $Z_{D4}$ | 0.4 + j 0.4 Ω |
| $Z_{D5}$ | 0.4 + j 0.4 Ω |
| **Load ratings** | |
| $Load_1$ | 13.3 kW and 7.75 kVAr |
| $Load_2$ | 11.2 kW and 6.60 kVAr |
| $Load_3$ | 27.0 kW and 7.0 kVAr |
| $Load_4$ | 23.2 kW and 6.1 kVAr |
| **DG ratings (nominal)** | |
| DG-1 | 30 kW |
| DG-2 | 20 kW |
| DG-3 | 20 kW |
| **Output inductances** | |
| $L_1$ | 0.75 mH |
| $L_2$ | 1.125mH |
| $L_3$ | 1.125mH |
| **DGs and VSCs** | |
| DC voltages ($V_{dc1}$ to $V_{dc4}$) | 0.220 kV |
| Transformer rating | 0.220 kV/0.440 kV, 0.5 MVA, 2.5% ($L_f$) |
| VSC losses ($R_f$) | 1.5 Ω |
| Filter capacitance ($C_f$) | 50 μF |
| Hysteresis constant (h) | $10^{-5}$ |
| **Droop Coefficients** **Angle-Real Power** | |
| $m_1$ | 7.5 rad/MW |
| $m_2$ | 11.25 rad/MW |
| $m_3$ | 11.25 rad/MW |
| **Voltage–Reactive Power** | |
| $n_1$ | 0.001 kV/MVAr |
| $n_2$ | 0.0015 kV/MVAr |
| $n_3$ | 0.0015 kV/MVAr |

## IV. SIMULATION STUDIES

Simulation studies are carried out in PSCAD/EMTDC (version 4.2). Different configurations of load and power sharing of the DGs are considered. To consider the web based communication, a delay of 5 ms is incorporated in the control signals which are not locally measureable. Since a single measurement is taken per each main cycle, a 100 byte/s communication is needed. This is a very low speed communication compared to any of the high bandwidth communication. The system parameters are shown in Table-I. For clarity, the numerical values of power sharing ratios obtained from all the simulation are given in Table-II.

*Case 1: Load_3 and Load_4 Connected to Microgrid*

In this case, all the three DGs are connected to the microgrid and supplying only Load_3 and Load_4. While the system in steady state, Load_3 is disconnected at 0.5 s. Fig. 7 (a) shows the power output of the DGs and Fig. 7 (b) shows the power sharing ratios with conventional angle controller given by (2). In Fig. 7 (b), $P_{ratio\text{-}ij}$ indicates $P_i{:}P_j$. It can be seen that due to high line impedance, the power sharing of the DGs are not as desired (see Table-II). Fig. 8 shows the system response with proposed Controller-1 discussed in Section II.A. The error in power sharing is reduced. Fig. 9 shows the system response with proposed Controller-2. The power sharing ratio of the DGs are much closer to the desired sharing and the system reaches steady state within 4-5 cycles as in the case with the conventional controller.

The results of this case with a conventional frequency droop controller are discussed in Appendix B.
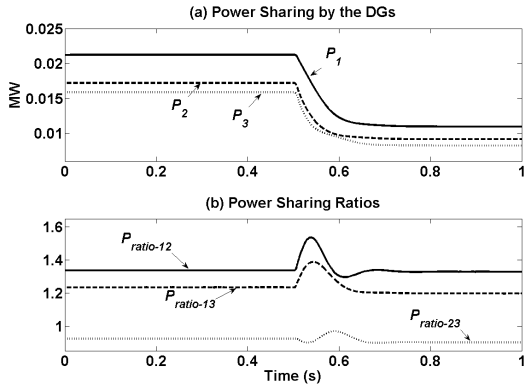


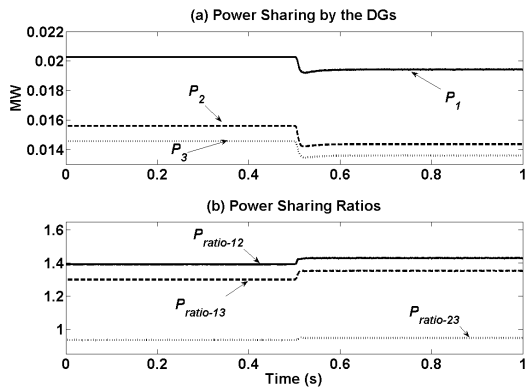Fig. 7. Power sharing with conventional controller (Case 1).



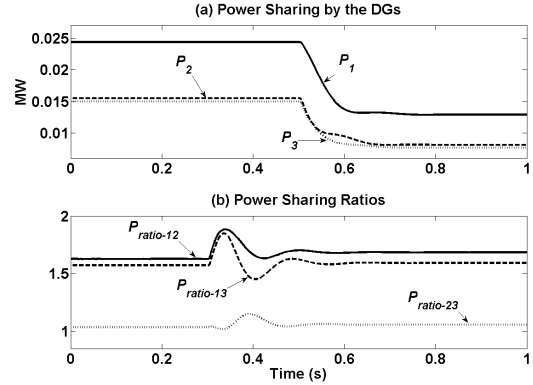Fig. 8. Power sharing with Controller-1 (Case 1).



Fig. 9. Power sharing with Controller-2 (Case 1).

*Case 2: DG-1 and DG-3 supply Load_1 and Load_2*

It is assumed that only two DG, DG-1 and DG-3 are connected to the microgrid and they are supplying Load_1 and Load_2. The system response shown in Fig 10 is with the conventional controller (2). Load_2 is disconnected at 0.5s and the two DGs, connected at the two ends of the microgrid supply only Load_1. Figs. 11 and 12 show the response with the proposed controllers. It can be seen that a closer to desired power sharing is achieved with these controllers. High line impedance (and high R/X ratio) between the DGs and load makes the power sharing difficult and the power sharing with conventional controller shown in Fig. 10 is not acceptable.
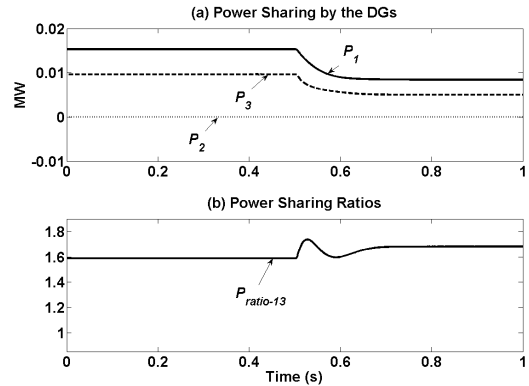


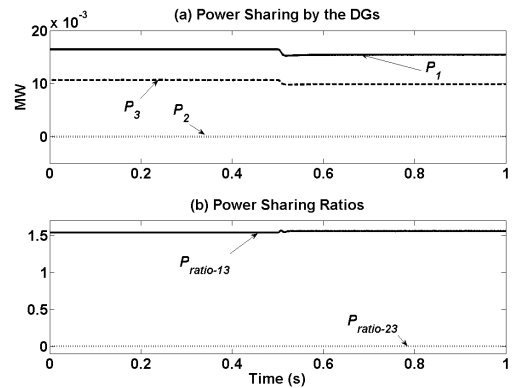Fig. 10. Power sharing with conventional controller (Case 2).



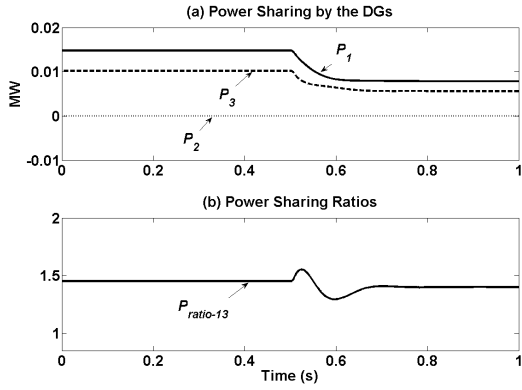Fig. 11. Power sharing with Controller-1 (Case 2).

Fig. 12. Power sharing with Controller-2 (Case 2).

## Case 3: Induction Motor Loads

To investigate the system response with induction motors connected to the microgrid, a 30 hp motor is connected as Load_3, while Load_4 constitutes a 50 hp motor. With the system running in steady state, DG-2 is disconnected at 0.25s. The simulation results are shown in Figs. 13 to 15 for the conventional controller and the two proposed controllers. After DG-2 is disconnected, DG-1 and DG-3 supply the total power demand and it can be seen that system takes around 0.3 s to reach the steady state. Due to the high impedance of the line, conventional angle controller fails to share the power as desired (error is almost 20%). Controller-1 reduces the error to some extent but not able to share as desired (Fig. 14 (b)). However, Controller-2 is able to share the induction machine load almost in the desired ratio (error is less than 2%).
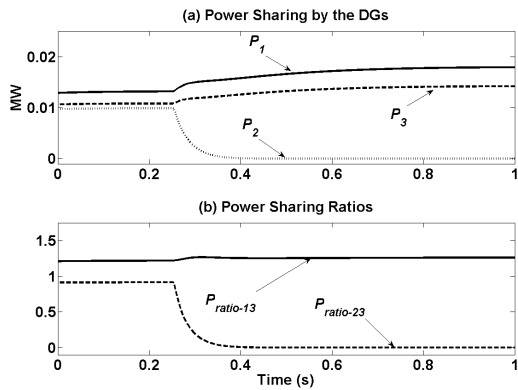


Fig. 13. Power sharing with conventional controller (Case 3).

## Case 4: Load Sharing with Advanced Communication System

In this section it is assumed that the system has advanced high bandwidth communication among all the DGs and loads and all the control parameters are measurable without any significant time delay. With the same induction motor load as in Case 3, the simulations are carried out considering all the measured variables are accessible to all the DGs. In this case, the droop sharing becomes redundant. Fig. 16 shows the system response. It can be seen that an accurate power sharing is achieved. The error is less than 0.5%. However the cost involved in a high bandwidth communication is much larger compared to the proposed no-communication or web based

minimum communication control. From this perspective, either Controller-1 or Controller-2 can provide an acceptable power sharing in a rural area with potentially a much lower cost.
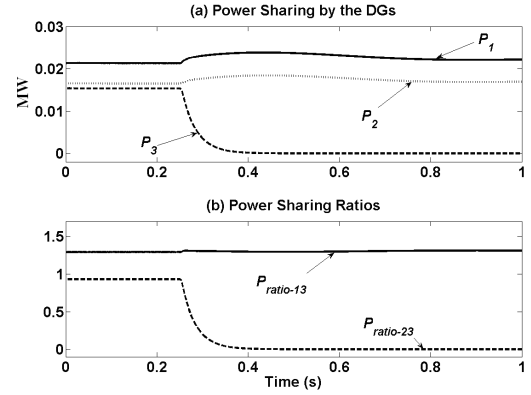


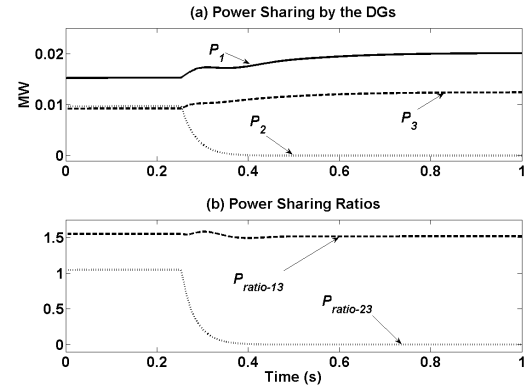Fig. 14. Power sharing with Controller-1 (Case 3).



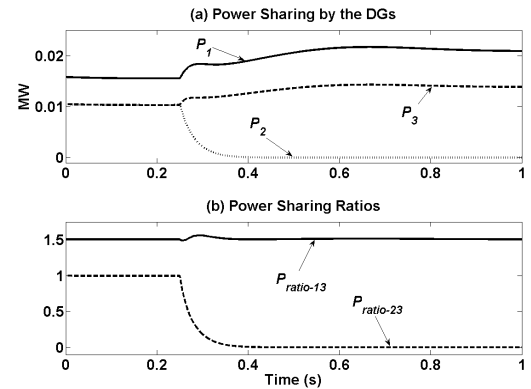Fig. 15. Power sharing with Controller-2 (Case 3).



Fig. 16. Power sharing with high bandwidth communication (Case 4).

Fig. 17 shows the mean percentage error in the different control techniques for the cases discussed above. The operating cases were chosen for weak system conditions, where the micro sources and loads are not symmetrically distributed through out the network. These results in high values of power sharing error but it can be seen that with the proposed control methods, the error can be reduced significantly. While the first proposed method (Controller-1) can reduce the error below 10%, the web based minimum communication method (Con-

troller-2) has an error around 3.5%. Though the error in case with an advanced communication system is much lower, the cost involved is likely to be high.

The decentralized droop sharing control has also been studied when the loads are voltage and frequency dependent. The results are discussed in Appendix C.

## V. CONCLUSIONS

Load sharing in an autonomous microgrid through angle droop control is investigated in this paper with special emphasis on highly resistive lines. Two control methods are proposed. The first method proposes power sharing without any communication between the DGs. The feedback quantities and the gain matrixes are transformed with a transformation matrix based on the line resistance-reactance ratio. The second method is with minimum communication based output feedback controller. The converter output voltage angle reference is modified based on the active and reactive power flow in the line connected at PCC. It is shown that a more economical and proper power sharing solution is possible with the web based communication of the power flow quantities. In many scenarios, the difference in error margin between proposed control schemes and a costly high bandwidth based communication system does not justify considering the increase in cost. This paper proposes and demonstrates low cost control methods to ensure acceptable power sharing in a weak system condition and highly resistive network for rural distribution networks.
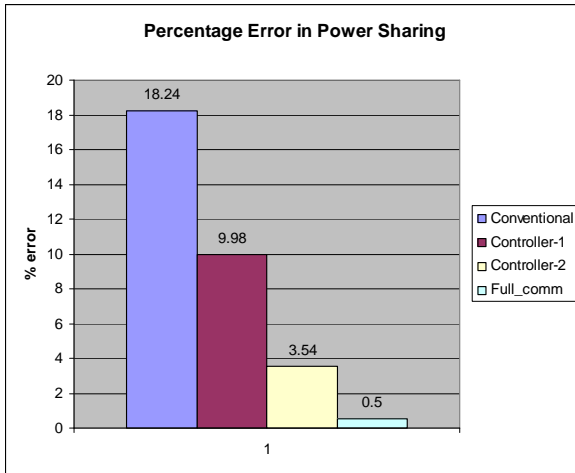


Fig. 17. Error in power sharing with different control techniques

TABLE-II: SIMULATION RESULTS

| Case | Controller | Power Sharing Ratio | | | | | |
| | | $P_1/P_2$ | | $P_1/P_3$ | | $P_2/P_3$ | |
| | | Initial | Final | Initial | Final | Initial | Final |
| 1 | Desired Values | 1.5 | 1.5 | 1.5 | 1.5 | 1.0 | 1.0 |
| | Conventional | 1.32 | 1.3 | 1.22 | 1.2 | 0.62 | 0.59 |
| | Controller-1 | 1.39 | 1.41 | 1.31 | 1.37 | 0.71 | 0.72 |
| | Controller-2 | 1.59 | 1.6 | 1.53 | 1.54 | 1.02 | 1.03 |
| 2 | Desired Values | – | – | 1.5 | 1.5 | – | – |
| | Conventional | – | – | 1.60 | 1.69 | – | – |
| | Controller-1 | – | – | 1.55 | 1.58 | – | – |
| | Controller-2 | – | – | 1.48 | 1.46 | – | – |
| 3 & | Desired Values | – | – | 1.5 | 1.5 | 1.0 | 0.0 |
| | Conventional | – | – | 1.22 | 1.25 | 0.97 | 0.0 |
| 4 | Controller-1 | – | – | 1.39 | 1.42 | 1.10 | 0.0 |
| | Controller-2 | – | – | 1.52 | 1.51 | 1.02 | 0.0 |
| | Full comm | – | – | 1.51 | 1.51 | 0.99 | 0.0 |

## REFERENCES

[1] M. C. Chandorkar, D. M. Divan and R. Adapa, "Control of parallel connected inverters in standalone ac supply systems," IEEE Trans. On Industry Applications, Vol. 29, No. 1, pp. 136-143, 1993.

[2] R. Majumder, A. Ghosh, G. Ledwich and F. Zare, "Load sharing and power quality enhanced operation of a distributed microgrid," IET Renewable Power Generation, Vol-2, No-3, pp 109-119, June, 2009, Current Issue, web http://www.ietdl.org/IET-RPG.

[3] M. N. Marwali, M. Dai; A. Keyhani, "Robust stability analysis of voltage and current control for distributed generation systems" IEEE Trans. on Energy Conversion, Vol. 21, Issue-2, pp. 516-526, 2006.

[4] M. Reza, D. Sudarmadi, F. A. Viawan, W. L. Kling, and L. Van Der Sluis, "Dynamic Stability of Power Systems with Power Electronic Interfaced DG," Power Systems Conference and Exposition, PSCE'06, pp. 1423-1428, 2006.

[5] J. G. Slootweg and W. L. Kling, "Impacts of distributed generation on power system transient stability," Power Engineering Society Summer Meeting, 2002 IEEE Vol. 2, No. , pp. 862-867, 2002.

[6] A.P. Agalgaonkar; S.V. Kulkarni, S.A. Khaparde, "Evaluation of configuration plans for DGs in developing countries using advanced planning techniques," IEEE Trans. on Power Electronics, Vol. 21, No. 2, pp. 973-981, 2006.

[7] B. K. Blyden and W.J. Lee, "Modified Microgrid Concept for Rural Electrification in Africa", Power Engineering Society General Meeting, pp. 1-5, 2006.

[8] K. D. Brabandere, B. Bolsens, J. V. Keybus, A. Woyte, j. driesen and R. Belmans, "A Voltage and Frequency Droop Control Method for Parallel Inverters", *IEEE Trans. Power Electronics*, Vol. 22, No. 4, pp. 1107-1115, Oct. 2008.

[9] Australian Business Council Sustainable Energy, web http://www.bcse.org.au/home.asp.

[10] B. Qiu and H. Gooi, "Web-based SCADA display system (WSDS) for access via Internet," *IEEE Trans. Power Systems*, Vol. 15, pp. 681-686, May 2000.

[11] N. Liu, J. Zhang, and W. Liu, "A security mechanism of web services-based communication for wind power plants," *IEEE Trans. Power Delivery*, Vol. 23, pp. 1930-1938, Oct. 2008.

[12] S.-J. S. Tsai and C. C. Luo, "Synchronized Power-Quality Measurement Network With LAMP," *IEEE Trans. Power Delivery*, Vol. 24, No. 1, pp. 484-485, Jan. 2009.

[13] Power System Load Flow Analysis, Lynn Powell, ISBN13: 9780071447799, McGraw-Hill Professional Publishing, November 2004

[14] A. Ghosh and A. Joshi, "A new approach to load balancing and power factor correction in power distribution system," IEEE Trans. on Power Delivery, Vol. 15, No. 1, pp. 417-422, 2000.

[15] A.Ghosh and G. Ledwich, *Power Quality Enhancement using Custom Power Devices*, Kluwer's Power Electronics and Power System Series, Kluwer's Academic Publishers, Norwell, MA, 2002.

[16] P. Kundur, Power System Stability and Control, McGraw Hill, 1994.

## APPENDIX-A

In this appendix, the comparison between the angle and frequency droop [1] is presented. The simple system, as shown in Fig. 1, is considered. The output impedances of the two sources are chosen in a ratio of 1:1.33 and the power rating of the DGs are also chosen in the ratio of 1.33:1. To investigate the frequency deviation, the load conductance is chosen as the integral of a Gaussian white noise source with zero mean and standard deviation of 0.01 Mho. The controllers are designed

ensuring same stability margin. The DG-1 power output and the operating frequency are shown in Fig. 18. It can be seen that the frequency deviation with frequency droop is much large than that with the angle droop. Since the output voltages in the two cases are chosen to be same (1 kV) and the output power shown in Fig. 18 is also similar, there is no difference in the converter requirements for the two droop controllers.
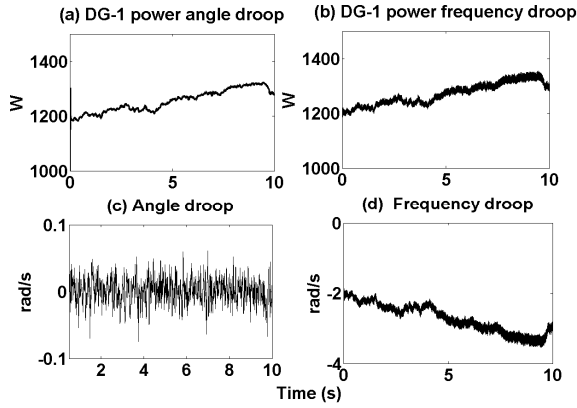


Fig. 18. Frequency droop and angle droop

APPENDIX -B

The performance of the conventional frequency droop controller for the high R/X system of Case 1 is shown in Fig. 19. It can be seen, as is in the case of the conventional angle droop performance seen in Fig. 7, the power sharing with this frequency droop is far from desired.
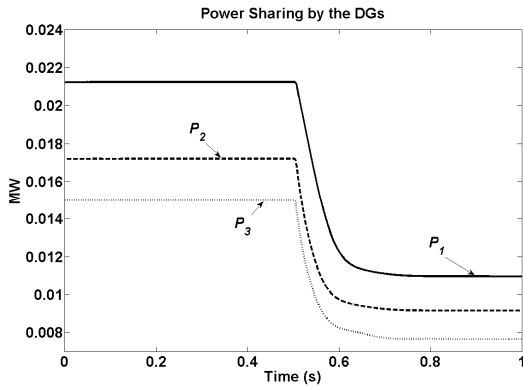


Fig. 19. Power sharing with frequency droop Case 1.

APPENDIX -C

To investigate the angle control performance with a frequency (F) and voltage (V) dependent load, a system as shown in Fig. 1 is chosen with a load perturbation as mentioned in Appendix B. The dependent load characteristic [16] is given by

$$P = P_0 \left( \frac{V}{V_0} \right)^{NP} \left( 1 + K_{PF} dF \right) \qquad (A.1)$$

where $NP$ (0.95) and $K_{PF}$ (2.0) are the voltage and frequency dependent coefficients. The system is initially running with a continuous varying impedance load. Then the dependent load

described by (A.1) is connected at 0.4s. The power sharing is shown in Fig. 20 (a). The system frequency and the power demand from the frequency dependent load is shown in Fig. 20 (b-c). It can be seen that the power sharing is as desired. However the droop gains may need to be reduced as the frequency dependence of the loads can be destabilizing.
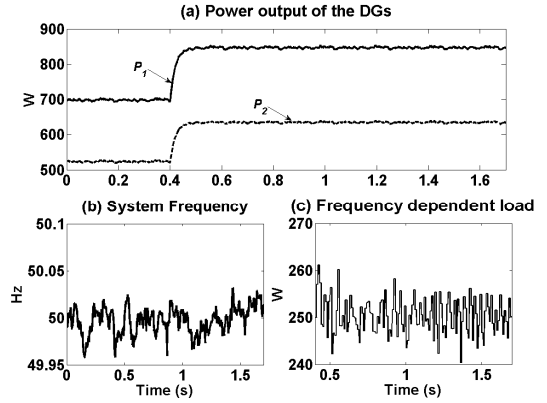


Fig. 20. Frequency dependent load

**Ritwik Majumder** (S'07) received his B.E. in Electrical Engineering from Bengal Engineering College (Deemed University) in 2001 and his M.Sc. (Engg.) degree from Indian Institute of Science in 2004. From 2004 to 2007, he worked with Tata Motor Engineering Research Centre, India, Siemens Automotive India and ABB Corporate Research Centre, India. Since June 2007, he is a Ph.D. scholar in Queensland University of Technology. His interests are in Power Systems dynamics, Distributed Generation and Power Electronics Applications.

**Gerard Ledwich** (M'73, SM'92) received the Ph.D. in electrical engineering from the University of Newcastle, Australia, in 1976. He has been Chair Professor in Power Engineering at Queensland University of Technology, Australia since 2000. His interests are in the areas of power systems, power electronics, and controls. He is a Fellow of I.E. Aust.

**Arindam Ghosh** (S'80, M'83, SM'93, F'06) is the Professor of Power Engineering at Queensland University of Technology, Brisbane, Australia. He has obtained a Ph.D. in EE from University of Calgary, Canada in 1983. Prior to joining the QUT in 2006, he was with the Dept. of Electrical Engineering at IIT Kanpur, India, for 21 years. He is a fellow of Indian National Academy of Engineering (INAE) and IEEE. His interests are in Control of Power Systems and Power Electronic devices.

**S. Chakrabarti** (S'06, M'07) obtained the Ph.D. degree in Electrical Engineering from Memorial University of Newfoundland, Canada, in 2006. Currently he is working as a Lecturer in the School of Engineering Systems, Queensland University of Technology, Brisbane, Australia. His research interests include power system dynamics and stability, state estimation, and renewable energy systems.

**Firuz Zare** (M'97, SM'06) was born in Iran in 1967. He holds a PhD degree in Electrical Engineering from Queensland University of Technology in Australia. He has worked as a development engineer and a consultant in industry for several years. He has joined the school of engineering systems in QUT in 2006. His research interests are power electronic applications, pulse-width modulation techniques, renewable energy systems and electromagnetic interferences.